

Infrared Spectroscopic Observations of the Secondary Stars of Short Period Cataclysmic Variables

Ryan T. Hamilton, Thomas E. Harrison

New Mexico State University

Department of Astronomy, PO Box 300001, MSC 4500, Las Cruces, NM 88003

`rthamilt@nmsu.edu`, `tharriso@nmsu.edu`

and

Claus Tappert

Universidad de Valparaiso

Valparaiso, Chile

`ctappert@astro.puc.cl`

and

Steve B. Howell

NOAO

950 N. Cherry Avenue, Tucson, AZ 85726

`howell@noao.edu`

Received _____; accepted _____

ABSTRACT

We present K -band spectroscopy of short period, “sub-gap” cataclysmic variable (CV) systems obtained using ISAAC on the VLT. It is extremely difficult to see the secondary stars in short period systems, since the low luminosity secondaries are swamped by the accretion disks in these objects. We show the infrared spectra for 9 systems below the gap: V2051 Oph, V436 Cen, EX Hya, VW Hyi, Z Cha, WX Hyi, V893 Sco, RZ Leo, and TY PsA. We are able to clearly detect the secondary star in all but WX Hyi, V893 Sco, and TY PsA. We present the first direct detection of the secondary stars of V2051 Oph, V436 Cen, and present new detections and revised spectral types for EX Hya, VW Hyi, Z Cha, and RZ Leo.

Subject headings: cataclysmic variables — infrared: stars — stars: abundances

1. Introduction

Cataclysmic variables (CVs) are short-period binaries in which a late-type, Roche-lobe filling star transfers matter through an accretion disk onto a rotating, accretion heated white dwarf (WD). The standard evolutionary paradigm (Howell et al. 2001, “HNR”) states that an intermediate mass primary and a low mass secondary starts life as a wide binary. As the primary star evolves off the main sequence, a common envelope binary is formed and the orbit shrinks as the secondary star interacts with the red giant envelope. A contact binary is then formed, and mass transfer begins between the primary and the secondary stars. During this time it is believed that angular momentum is lost through a magnetically constrained wind (“magnetic braking”, see Collier Cameron 2002, and references therein), keeping the secondary in contact with its Roche lobe as it continues to lose mass. As time passes, the secondary star is slowly whittled away, and its mass decreases. HNR show that during this time, the secondary stars in CVs are bloated because they are out of equilibrium, and do not follow a main sequence mass-radius relationship.

Eventually, the secondary stars attain low enough masses that they become fully convective, and at this point it is believed that the magnetic braking ceases, the secondary star returns to its equilibrium radius, and loses contact with its Roche surface. This is the origin of the “period gap”, the fact that very few CVs are found with orbital periods between two and three hours. Inside the period gap, angular momentum is believed to be lost via gravitational radiation, and the orbital period decreases very slowly, until contact recurs at $P_{\text{orb}} = 2$ hr, at which point the binary emerges as a “sub-gap” CV.

Under the standard evolutionary paradigm, the secondary stars of CVs are expected to be relatively normal main sequence-like objects. An infrared spectroscopic survey of non-magnetic CVs by Harrison et al. (2004, 2005) found, however, that the CO features of the secondary stars in most systems were much weaker than they should be for their

spectral types. Since the water vapor features in the coolest of these stars appeared to be normal, this result indicated a deficit in carbon. In addition, some of the spectra also suggested that ^{13}C was enhanced. It had long been noticed (e.g., Bonnet-Bidaud & Mouchet 1987, Szkody & Silber 1996, Mauche et al. 1997) that the N V to C IV ratio in the Ultraviolet (UV) spectra of a number of cataclysmic variables was very high, suggesting a strong enhancement of nitrogen, and/or a deficit of carbon in the accretion disk, or in the WD photosphere.

In contrast, the majority of “polars”, CVs with highly magnetic WD primaries, have secondary stars that appear to be completely normal (Harrison et al. 2007). UV spectroscopy of a large sample of polars by Arajou-Betancor et al. (2004) showed that these polars also had normal N V/C IV line ratios. The implication of this set of observations is that the matter transferred from the secondary star in non-magnetic systems is the source of the UV abundance anomalies, and that these stars have CNO processed material in their atmospheres. It is important to note that when complementary data exists, every CV that shows weak CO absorption features in the K -band appears to have a C deficit, and enhanced levels of N, in UV spectra.

This result is further strengthened by two exceptions to the above trends: SS Aur and V1309 Ori. Howell et al. (2010) present K -band spectra of both SS Aur and V1309 Ori. SS Aur is a typical dwarf nova above the period gap ($P_{\text{orb}} = 4.26$ hr), while V1309 Ori is the longest period ($P_{\text{orb}} = 7.98$ hr) polar. The secondary star in SS Aur appears to have normal CO features, while V1309 Ori has extremely weak CO features. Analysis of the UV spectra of SS Aur by Godon et al. (2008) show that it has normal C and N abundances. It has been known for a while (Schmidt & Stockman 2001) that V1309 Ori showed highly anomalous N emission. The correlation between the CO features in the secondary star, and the abundances derived from UV spectra, is so strong that it appears that one can now be

used to predict the other.

Howell et al. (2010) discuss the various scenarios that one might attempt to use to explain away these results, but none of them can simultaneously explain the strong UV/IR correlation. As we discuss below, the standard paradigm for CV evolution probably needs to be revised to account for these results. It is important in this context, however, to point out the fact that the majority of the non-magnetic CVs so far observed in the infrared are above the period gap, while the majority of the polars are below the period gap. Thus, there could be different evolutionary paths for systems above the gap, and those below. The question that needs to be answered is: what do non-magnetic CV secondaries in sub-gap systems look like?

A large sample of moderate resolution infrared spectroscopy for systems below the period gap does not exist in the literature. The very low luminosities expected for the secondary stars in short period CVs has a difficult time competing with the accretion luminosity, making these objects difficult to detect. Ishioka et al. (2007) used the Subaru Telescope to obtain J , H , and K -band low resolution grism spectroscopy of five CVs below the gap. Spectral energy distribution (SED) fitting allowed them to obtain spectral type estimates ranging from M1 to L1. The low resolution of these data ($\text{FWHM} \sim 60\text{\AA}$) prevented examination of the CO features. Harrison et al. (2009) obtained moderate resolution observations of two short period systems, VY Aqr and EI Psc. There is strong evidence for a hot K-type secondary in EI Psc (Thorstensen et al. 2002), unexpected given its ultra-short period ($P_{\text{orb}} = 1.07$ hr). It should have a very late type companion, but the IR spectroscopy confirms the mid-K spectral type, and reveals a secondary star with extraordinarily weak CO features. The results for VY Aqr ($P_{\text{orb}} = 1.51$ hr) were not as clear, as the spectral type of the secondary star derived from the VLT (\sim M6) and Keck (\sim M0) data sets were quite different. No matter the classification, the CO features in the

secondary star of VY Aqr were extremely weak.

To attempt to detect the secondary stars in a sample of sub-gap CVs, we have obtained moderate resolution K -band spectra of eight sub-gap CVs using ISAAC on the VLT. We clearly detect the presence of the secondary star in seven of these systems. In contrast to the longer period CVs, the majority of these secondary stars have CO features that appear to be present at near-normal strengths. We present our observations in Section 2, the object spectra and spectral type determinations in Section 3, a discussion of our results in Section 4, and our conclusions in Section 5.

2. Observations

Infrared spectroscopy for the program objects (see Table 1) was carried out at the European Southern Observatory (ESO) in Cerro Paranal, Chile, with the the Infrared Spectrometer And Array Camera (ISAAC) (Moorwood et al. 1998) on the 8.2 meter Very Large Telescope (VLT) Antu in service mode between May and August of 2008. Additional infrared data were obtained for both RZ Leo and EX Hya utilizing NIRSPEC (McLean et al. 1998) at the W. M. Keck Observatory at Mauna Kea.

2.1. VLT Antu

The ISAAC data were obtained in the standard infrared ABBA nodding pattern, moving the object between two positions on the spectrograph slit to aid in the removal of sky background. A detailed observation log is given in Table 1, listing the observation dates and times for each system, the exposure times and the number of observations at each nodded position, and the percentage of the orbital phase covered in the observation set. These data were taken using a medium resolution grating and a $0.6''$ slit, giving a resolving

power of $R \sim 4400$ and a dispersion of $1.20 \text{ \AA pixel}^{-1}$ across the 1024 pixel square ISAAC science CCD. We used two wavelength centers to cover the red end of the K -band, one centered on $2.25 \text{ }\mu\text{m}$ and another centered at $2.35 \text{ }\mu\text{m}$, giving sufficient overlap to construct a composite spectrum covering 2.18 to $2.40 \text{ }\mu\text{m}$. The observing conditions varied during the observation period but, in general, these data were obtained in fair conditions with seeing generally less than $1.25''$ as reported by the Differential Image Motion Monitor (DIMM) at the VLT.

Several problems appeared during the observation run, however, that impacted the quality of these data. Several large dust particles appeared on the detector, degrading the cosmetics and compromising the spectral extraction. This specifically impacted the data for V436 Cen and V893 Sco. In addition to this, significant drift in the central wavelength positions were observed, particularly if the center position was changed before, or after, a telluric standard was observed. Using night sky lines as a wavelength calibration source mitigated this effect, but in general telluric correction and wavelength calibration were more challenging than expected. The final, reduced VLT spectra for our program objects are shown in Fig. 1.

2.2. Keck Observatory

Both EX Hya and RZ Leo were observed using NIRSPEC at the W. M. Keck Observatory, using a $0.380''$ slit and a low resolution grating covering approximately 2.04 to $2.46 \text{ }\mu\text{m}$ with a dispersion of $4.27 \text{ \AA pixel}^{-1}$. These data were obtained in the standard infrared ABBA nodding pattern, and reduced using the IDL routine REDSPEC¹. The data reduction process followed the description given in Harrison et al. (2005a). Both objects had telluric corrections applied in REDSPEC using observations of featureless A0 V stars close to the program objects to remove atmospheric absorption lines, and to avoid any

differences in telluric absorption dependent on airmass. We used arc lamps to provide a wavelength calibration. The spectrum for RZ Leo has been presented in Howell et al. (2010), but we include it here to compare it to our results for the other sub-gap systems. The final, reduced spectrum of RZ Leo is included in Fig. 1, where only the VLT spectrum of EX Hya is shown.

2.3. Reductions

Standard data reductions were carried out using ESO GASGANO¹ interface and the Common Pipeline Library (CPL) using the ISAAC reduction recipes version 5.7.0. The reduction recipes were executed using the GASGANO interface. The pipeline obtains a wavelength calibration by examining the night sky lines in each data frame, and corrects for field curvature using arc lamp frames collected at the end of each night as well as dividing by a flat field. It then detects the spectrum present in each input frame, shifting and co-adding to produce only one output. Modifications were made to this pipeline to output the individual corrected frames, which could then be properly combined to account for the significant radial velocity variations of the secondary star. While we were able to obtain a good corrected spectrum for each system, the resulting radial velocity curves were extremely noisy and are not shown here. The modifications to the CPL recipes were checked for accuracy by also examining the data with standard IRAF² methods (*apall*, *identify*, etc.) and found to give indistinguishable results. Telluric features were removed using nearby A0V standard stars observed close to the same airmass of the program objects. Telluric standard stars were in general observed at the end of each night, within ± 0.2

¹Details about the REDSPEC IDL package can be found on-line at the instrument website at <http://www2.keck.hawaii.edu/inst/nirspec/redspeg.html>.

airmasses of the program objects. In most cases only one telluric standard was observed each night. These followed the same reduction process as the data frames, but instead used the single combined output from the reduction pipeline since radial velocity smearing was not an issue. The most appropriate standard was then divided into the observation using the IRAF task *TELLURIC*, which allows scaling and shifting the standard to best match the atmospheric absorption lines present in the data. Care was taken to not scale or shift the standard too much and introduce spurious absorption or emission lines in these data.

2.4. M Star Templates

In addition to the spectra of the CVs, we obtained spectra of three late-type dwarf templates. Each reference object was compared against standards taken from the IRTF Spectral Library (Cushing et al. 2005) as a check on the spectral reductions, and the spectral types we derive are consistent with those reported in the SIMBAD database. The observing log of the M stars observed as part of our program can be found in Table 1. When necessary, these three M star templates were supplemented with additional, lower resolution ($R \sim 2,000$) spectra from the IRTF Spectral Library.

²<http://www.eso.org/sci/data-processing/software/gasgano/>

³IRAF is distributed by the National Optical Astronomy Observatories, which are operated by the Association of Universities for Research in Astronomy, Inc., under cooperative agreement with the National Science Foundation

3. Results

In the following, we attempt to assign spectral types to the secondary stars of our program objects if they are clearly visible. The best indicator of the spectral type for late type dwarfs in the K -band is the ratio between the Na I doublet at $2.207\ \mu\text{m}$ and the Ca I triplet at $2.263\ \mu\text{m}$. As effective temperature decreases from M0, the Na I doublet gets stronger and the Ca I triplet gets weaker. The accretion disks in these systems are bright, and provide a flat power-law continuum that veils the absorption lines from the secondary star making a direct visual comparison to template spectral types as described in §2.4 more difficult. To overcome this, prior work (Mennickent & Diaz 2002; Mennickent et al. 2004; Ishioka et al. 2007) has focused on component fitting a range of stellar template spectra with a power law component to represent contributions from the disk to the J , H , and/or K band observations.

As a prelude to more in-depth synthetic spectral modeling currently underway, we take a more simplistic approach to get first estimates of the spectral types of the secondary stars visible in these data. We have used the IRAF task *CONTINUUM* to flatten both our program objects and our standard comparison spectra, allowing us to then scale each standard spectrum with a multiplicative constant that best matched each CV spectrum to determine the spectral type of the secondary. The continuum between the Na I doublet and the Ca I triplet is relatively free of other contaminating sources, so we are confident that the lines are undistorted by this process. The CO bandheads, however, could be compromised by the continuum fitting process as noted in Tappert et al. (2007) due to the presence of strong water vapor absorption at $\lambda \geq 2.28\ \mu\text{m}$. This very broad feature depresses the continuum, making it difficult to ascertain its true level in the fitting process.

3.1. V2051 Oph

V2051 Oph ($P_{orb} = 1.498$ hr) is an SU UMa type CV, exhibiting super-outbursts approximately every 227 days. It is also an eclipsing system, and was observed by Baptista et al. (1998) using both ground based photometry as well as *HST* FOS spectroscopy. Baptista et al. derived a secondary mass of $M_2 = 0.15 \pm 0.03 M_\odot$, and a radius of $R_2 = 0.16 \pm 0.01 R_\odot$, but gives no estimate of the secondary spectral type. They do speculate, however, that the system must be relatively young since the secondary does not seem to be out of thermal equilibrium. The empirical CV donor sequence by Knigge (2006) suggests that the secondary star of V2051 Oph should have a spectral type near M7. The 2MASS Point Source Catalog⁴ lists V2051 Oph as having $K_{2MASS} = 13.53$.

The ISAAC spectrum of V2051 Oph is presented in Fig. 2. This spectrum shows that the first overtone CO feature is stronger than the Na I doublet, suggesting a very late spectral type. The Ca I triplet is also not clearly detected, as would be expected if the secondary had a late-M spectral type. From comparison of its spectrum to the templates we derive a spectral type of $M7 \pm 1$ for V2051 Oph. The secondary of V2051 Oph has not been previously detected, thus this spectrum provides the first constraints on its nature.

3.2. V436 Cen

V436 Cen ($P_{orb} = 1.500$ hr) is an SU UMa type CV, exhibiting super-outbursts approximately every 630 days. It has been suggested (Patterson 2001; Knigge 2006) that V436 Cen could harbor a low mass secondary based on empirical fits to a relationship between the mass ratio q and the superhump and orbital periods. Ritter & Kolb (2003, update 7.12) report a secondary mass of $M_2 = 0.17 M_\odot$, but list it as an uncertain result.

⁴<http://www.ipac.caltech.edu/2mass/releases/allsky/doc/explsup.html>

The relationship in Knigge (2006) predicts an M7 dwarf donor. In quiescence, V436 Cen has $K_{2\text{MASS}} = 13.53$.

The spectrum of V436 Cen, shown in Fig. 2, appears to be slightly later than that of V2051 Oph. Using the Na I, Ca I, and CO features we derive a spectral type of $\text{M}8 \pm 1$. The data reduction process for this object was somewhat hampered by the lack of a good telluric standard to correct its spectra. As with V2051 Oph, this is the first direct detection of the secondary in V436 Cen.

3.3. EX Hya

EX Hya is a bright ($K_{2\text{MASS}} = 11.69$), well studied short period ($P_{\text{orb}} = 1.638$ hr) Intermediate Polar (IP), and is the only magnetic CV in our sample. Beuermann & Reinsch (2008) used optical spectroscopy and a previously derived value of K_1 to model the system, finding the mass of the secondary to be $M_2 = 0.108 \pm 0.008 M_{\odot}$, and a radius of $R_2 = 0.1516 \pm 0.0034 R_{\odot}$. They assigned a spectral type of $\text{M}5.5 \pm 0.5$ on the basis of Na I and TiO band strengths compared to M4V and M6V templates. *JHK* spectra of EX Hya during outburst were presented by Harrison et al. (2010), who noted that both water vapor absorption (at 1.38 and 1.9 μm) and the Na I doublet at 2.2 μm were visible even though EX Hya was two magnitudes brighter than it is at quiescence.

We have observed this system in quiescence with both ISAAC at the VLT, and with NIRSPEC (McLean et al. 1998) at the Keck Observatory. Both of these spectra are presented in Fig. 3, where we compare them to the spectra of two M dwarfs. In both datasets, the secondary star was prominent. The strength of the Ca I triplet in this system indicates an earlier spectral type than either of our first two objects. We derive a spectral type of M5 for this secondary star. In contrast to its longer period IP cousins, GK Per and

AE Aqr (see Harrison et al. 2007), EX Hya has CO absorption features that appear to be relatively normal. EX Hya has a high precision *HST* parallax (Beuermann et al. 2003) that gives a distance of 64.5 ± 1.2 pc. At this distance, an M5V would have $K = 12.57$, and would supply only 44% of the observed K -band flux.

3.4. VW Hyi

VW Hyi ($P_{orb} = 1.783$ hr) is an SU UMa type CV, with outbursts roughly every 28 days and super-outbursts approximately every 183 days. Mennickent et al. (2004) examined this system with ISAAC at low resolution, finding evidence for an $L0 \pm 2$ dwarf based on fitting of the J -band with a power-law disk component and a stellar template. Smith et al. (2006) estimate a primary mass of $M_1 = 0.71^{+0.18}_{-0.26} M_{\odot}$ from the gravitational redshift of the Mg II $\lambda 4481$ absorption line on the white dwarf. A mass ratio of $q = 0.148 \pm 0.004$ from the superhump-period excess (Patterson (1998)) predicts a secondary mass of $M_2 = 0.11 \pm 0.03 M_{\odot}$. Knigge (2006) predicts an M5 dwarf donor at this orbital period. VW Hyi is one of the brightest of the (non-magnetic) sub-gap CVs, having $K_{2MASS} = 11.70$.

Our spectrum of VW Hyi using ISAAC is shown in Fig. 3. The strength of the Na I doublet relative to that of the Ca I triplet point to a mid-M spectral type, and we find good agreement with an M4 dwarf. At this spectral type, the CO features are close to their expected strength. Strangely, the spectral region between 2.21 and 2.26 has a number of absorption features, which we tentatively associate with Fe I, that are much more consistent with a very late M-type dwarf (M9V). While the S/N of this spectrum is not particularly high, each of these features has the correct depth and width (as some are doublets), matching the features in the M9V. Later types, however, do not match the strengths of the other prominent spectral features, and we find that the spectrum is inconsistent with an L0 dwarf.

3.5. Z Cha

Z Cha ($P_{orb} = 1.788$ hr) is an SU UMa type CV, with recurrence times of ~ 17 days and ~ 287 days for normal and superoutbursts respectively. Wade & Horne (1988) observed Z Cha spectroscopically, and derived a radial velocity curve of the secondary star using the Na I doublet at $\lambda 8183$ and $\lambda 8194$, and combined that with a mass ratio of the system derived from eclipses by Wood et al. (1986) to derive system parameters of $M_1 = 0.84 \pm 0.09 M_\odot$ and $M_2 = 0.125 \pm 0.014 M_\odot$. Wade & Horne (1988) also find evidence for an M5.5 secondary star, based on TiO band strengths. Knigge (2006) predicts an M5 dwarf donor for this orbital period. Z Cha has $K_{2MASS} = 13.31$.

The spectrum of Z Cha using ISAAC is shown in Fig. 4. It must be noted that the blue portion of the spectrum was observed some 4 months *after* the redward side, as shown in Table 2. The AAVSO archive has magnitude estimates during both time periods, showing that the system was inbetween outbursts at the epochs of the VLT observations, with similar visual magnitudes. The spectrum is heavily contaminated by the accretion disk, making proper identification of the spectral type of the secondary star highly uncertain. If we accept the M5 classification, then the CO features are much weaker than they should be. This spectral type is consistent with the data given the observed strength of both the Ca I triplet and the Na I doublet.

3.6. V893 Sco

V893 Sco ($P_{orb} = 1.823$ hr) is an eclipsing system with $K_{2MASS} = 12.68$. Mason et al. (2001) obtained optical spectroscopy from which they derived an $H\alpha$ radial velocity curve consistent with $M_1 = 0.89 M_\odot$ and $q = M_2/M_1 = 0.19$, giving a secondary mass of $M_2 = 0.17 M_\odot$. Knigge (2006) predicts an M5 dwarf donor at this orbital period.

Thorstensen (2003) was able to measure the parallax of this system, putting the distance at 155^{+55}_{-34} pc. The Na I doublet and the first overtone of CO are visible in our spectrum of V893 Sco, but the quality of these data are low, and the Ca I triplet remains undetected. This spectrum does show a water vapor break, and this is indicative of a later type secondary than seen in Z Cha, and we suggest that the spectral type is $> M6$. An M6V at the distance of V893 Sco would have $K = 15.21$. Given that the secondary star is visible in the K -band suggests that V893 Sco is closer than given by the lower limit of the measured parallax.

3.7. RZ Leo

RZ Leo ($P_{orb} = 1.825$ hr) is a member of the small family of WZ Sge-like CVs, sometimes called “TOADs” (Howell et al. 1995), that exhibit infrequent, but very large (≥ 6 mag) SU UMa-type outbursts. Little information exists in the literature to date about the mass ratio or properties of either component in this system. Patterson et al. (2003) reports both an orbital and superhump period from spectroscopy and long term photometry of 1.82492 hrs and 1.888 hrs, respectively. Knigge (2006) estimates, under the assumption of a primary mass of $M_1 = 0.75 M_{\odot}$, a secondary mass of $M_2 = 0.114 M_{\odot}$ and a radius of $R_2 = 0.171 R_{\odot}$. The empirical CV donor sequence predicts an M5 dwarf at this orbital period.

The K -band spectrum of RZ Leo from NIRSPEC at Keck as described in §2.2 is shown in Figure 5. RZ Leo is the faintest of the objects in our survey (by two magnitudes), having $K_{2MASS} = 15.39$. Unlike the prototype TOAD WZ Sge, whose secondary has proved elusive, the donor star in RZ Leo is easily seen. It appears to be an $M4 \pm 1$ with normal CO features, based on the strengths of the Na I doublet and the Ca I triplet. This spectral type is similar to the M5 assigned by Mennickent & Diaz (2002) from SED fitting of lower

resolution ISAAC J , H , and K -band spectra.

3.8. WX Hyi and TY PsA

WX Hyi ($P_{orb} = 1.796$ hr) is an SU UMa type CV, and was first spectroscopically examined by Schoembs & Vogt (1981). Using optical spectroscopy, they found a primary mass of $M_1 = 0.9 \pm 0.3 M_\odot$ and mass ratio $q = M_1/M_2 = 5.5 \pm 1.5$ based on radial velocity fitting. Ritter & Kolb used these to estimate a secondary mass of $M_2 = 0.16 \pm 0.05 M_\odot$. We have been unable to find any other information about the possible spectral type of the secondary star. Even though it is relatively bright, $K_{2MASS} = 12.96$, no identifiable absorption features can be seen in its infrared spectrum (see Fig. 1). In fact, in contrast to every other object, it shows a slightly rising spectrum at the red end of the K -band.

TY PsA ($P_{orb} = 2.02$ hr) is a rarely studied SU UMa type CV. Prior spectroscopic examinations of this system (Warner et al. 1989; O’Donoghue & Soltynski 1992) found no radial velocity variations, suspecting that this system might has an extreme mass ratio and therefore a sub-stellar companion. Mennickent et al. (2004) examined this system in the infrared with ISAAC previously, and found no features of the secondary star. Knigge (2006) predicts an M4.5 dwarf donor at this orbital period. Unlike WX Hyi, the continuum for TY PsA shows a slight decline at the red end of its spectrum. Given the considerable contamination needed to wash-out the other absorption features, this would suggest a late spectral type ($> M6$) so as to have a large enough water vapor feature to affect the continuum. Given that it has an almost identical brightness to V2051 Oph ($K_{2MASS} = 13.58$ vs. 13.53), and we used the same exposure time as on that object, the 2MASS survey must have caught this object somewhat brighter than it is at true quiescence. Using our raw data shows that the count rate for TY PsA was only half that of V2051 Oph, suggesting that it has $K \approx 14.3$.

4. Discussion

We have conducted a moderate resolution spectroscopic survey of nine CVs below the period gap. We clearly detect features from the secondary stars in seven of these objects, and a suspected water vapor decline in an eighth object. All of the secondary stars appear to be mid- to late-type M dwarfs and are consistent with the measured/estimated masses available in the literature, or as might be expected using predictions from the empirical donor sequence of Knigge (2006). Our new spectral type estimates are plotted on the empirical donor sequence in Fig. 6 (blue circles). We have added our results (Harrison et al. 2009) for both EI Psc and VY Aqr to this diagram for completeness.

With the results of this diagram in hand, Knigge (2006) discussed how to use it to provide lower limits on the distance using single epoch K -band measurements. By combining our spectroscopically determined spectral types with the observed infrared photometry shows, however, that this procedure can only provide weak constraints on the distances to sub-gap CVs. In Fig. 7 we plot the 2MASS colors for our program objects, along with the main sequence color-color relationship. Two objects fall near the main sequence relationship: EI Psc, and RZ Leo. As discussed in Harrison et al. (2009) EI Psc ($P_{\text{orb}} = 1.07$ hr) acts just like a main sequence K5 dwarf in the infrared, and apparently suffers from very little accretion disk contamination. The other object, RZ Leo, has such uncertain photometry ($\sim \pm 0.2$ mags, see Table 3), that its colors are completely consistent with the main clump of objects in this diagram. The objects with the best-determined spectral types in our survey are V2051 Oph, V436 Cen, VW Hyi, and EX Hya. The first three of these objects have very similar colors (especially in $H - K$), but range from M8 (V436 Cen) to M4 (VW Hyi). This result suggests that there is substantial disk contamination occurring in both V2051 Oph and V436 Cen—yet these two objects have secondary stars that are just as easily seen as those in VW Hyi and EX Hya! Deconvolving

the infrared colors of CVs remains a difficult task, and infrared photometry should be used with caution when estimating *any* intrinsic parameter of these systems.

This conclusion is further strengthened by the two systems in our survey with measured parallaxes: EX Hya, and V893 Sco. Using the Knigge relationship for EX Hya, one derives a lower limit to its distance of $d = 30$ pc, while the parallax gives 62 pc. The relationship would predict a distance of 53 pc for V893 Sco versus the parallax measurement of 155 pc. Both of these limits are less than one half of what is measured, even accounting for the significant uncertainty in the parallax for V893 Sco. This is better demonstrated by assembling all of the published parallaxes for CVs (but excluding “polars”, and AM CVn systems) and deriving a $M_K - P_{\text{orb}}$ relationship (parallaxes from Harrison et al. 2004b, Thorstensen et al. 2008, and Thorstensen 2003). We show this result in Fig. 8. While there is clearly a lower limit on M_K that depends on P_{orb} , at any one orbital period the spread in M_K is *two magnitudes or more*.

4.1. The Strength of the CO Features and the Origin of the Period Gap

In contrast to our results for longer period CVs (Harrison et al. 2004a, 2005), the secondary stars of the majority of sub-gap systems in this survey do not show evidence for weaker than expected CO features. The two exceptions for which we have IR spectra are VY Aqr and Z Cha, though the spectrum of the latter object is not of sufficient quality to conclusively determine its spectral type. UV spectroscopy has shown, however, that at least three additional sub-gap systems show C deficits: BC UMa, SW UMa, and BW Scl (Gänsicke et al. 2005). In addition, UV spectroscopy of VW Hyi Sion et al. (1996) also suggested sub-solar C abundances. More recent analysis (E. Sion, private communication), however, suggests that the C abundance in VW Hyi is close to solar. One way to explain “normal” C abundances at short periods was demonstrated by Marks & Sarna (1998). For

their models where the secondary has evolved off of the main sequence before contact, they show that the surface C abundance in the secondary star declines throughout most of its life as a CV (see their Fig. 16) until its mass reaches $\sim 0.3 M_{\odot}$. After this point the surface C abundance returns to normal as material from deeper layers within the star, unaffected by the CNO cycle that operated prior to contact, are convected to the surface.

In our introduction, we asked the question whether sub-gap CVs were different from their longer period cousins: having a separate evolutionary path for short period CVs, as might be suggested by the normalcy of the secondary stars in polars. Given the results that abundance patterns in sub-gap CVs are not obviously different from the above-gap systems suggests that the period gap is not an artifact of different progenitors for long and short period CVs.

The standard paradigm for the formation of the period gap proposes that the secondary stars become fully convective near $P_{\text{orb}} = 3$ hrs (with masses near $0.23 M_{\odot}$; HNR), and that the magnetic braking, the dominant angular momentum loss mechanism, shuts down due to a change in the dynamo. As discussed by Andronov & Pinsonneault (2004), there is nothing “magical” about the angular momentum loss rate or stellar activity levels at the fully convective boundary. This result has only been strengthened with additional data for low mass stars in clusters (c.f., Scholz et al. 2009, and references therein). In fact, Donati et al. (2008) show that there is a dramatic *increase* in the dynamo generating processes at the fully convective boundary.

Given that becoming fully convective does not appear to be a reasonable method for producing the period gap, is there an alternative method for shutting down the magnetic braking? One possible method to offset the influence of the high levels of magnetic activity seen at the fully convective boundary, with the weaker magnetic braking observed for these stars, is to suppose that the field topology changes from a predominantly large scale

toroidal configuration seen in stars with radiative zones (see Solanki 2009), to a much more complex, nonaxisymmetric topology in fully convective stars. In this case, the global field might more closely resemble a collection of multi-polar structures whose individual field strengths fall off rapidly with distance, resulting in a much weaker global field. Such fields would have limited numbers of “open field” lines along which to transport material, and thus much lower magnetic braking (see Collier Cameron 2002). This idea has been shown not to be perfectly true by Donati et al. (2006) who demonstrate that V374 Peg, a rapidly rotating ($P_{rot} = 10.69$ hr), fully convective M4V has a large scale, axisymmetric poloidal field. A similar result was found for the M4 dwarf GL 490B by Phan-Bao et al. (2009). At the same time, however, there is strong evidence that the majority (85%) of the magnetic energy remains locked-away in smaller structures. Perhaps the factor of ~ 3 increase (compared to V374 Peg) in rotational velocity for CV secondaries at the top of the period gap is sufficient to eliminate the large scale poloidal field.

One characteristic of rapid rotating late-type stars is that much of the stellar activity is located closer to the poles of these objects (see Bushby 2003, and references therein). In some CVs polar spots are seen (Watson et al. 2006), while in others the spots are more equatorial (Watson et al. 2007). Cohen et al. (2009) show that if a spot is located near the pole, the stellar wind structure is dramatically affected, and that total mass and angular momentum loss is substantially higher than if the spots were equatorial. Unless it is found that the spots on CVs are preferentially located near the equatorial regions, this explanation seems unable to produce the desired result.

While observations of the magnetic field structures in low mass stars is improving, as is our understanding of the generation of their magnetic dynamos, the extension of this knowledge to explain the CV period gap remains elusive. Since there is one, and only one property that all CVs at the top of the period gap must share, their three hr rotation period,

it must be that rotation somehow quenches the efficient magnetic dynamo generation in fully convective stars.

5. Conclusions

Main conclusions: with sufficient resolution nearly all of these objects are visible! better quality data should allow us to get RV curves, and thus masses. while our results indicated a large normal CO fraction, we have insufficient objects to fully test this idea, and UV already says it is not absolute. rotation rate is what forms the period gap, but how remains unclear.

Ongoing analysis and modeling of our infrared spectra presented here will allow us to explore both the normal and weak CO bands seen in our spectra. In particular, we will fully assess the $^{12}\text{C}/^{13}\text{C}$ ratio which gives the best indication and possibility to see if the secondary star contains any CNO processed material, hinting at a much different evolutionary picture for the secondary stars of cataclysmic variables.

It is only through detailed and simultaneous analysis of both the infrared and ultraviolet data that the secondary donor star and the primary white dwarf can be disentangled. We are going to do that. [I know that last sentence is horrible but I thought I should put something in there.]

Based on observations made with ESO Telescopes at the La Silla or Paranal Observatories under program ID 081.D-0225.

Some of the data presented herein were obtained at the W.M. Keck Observatory, which is operated as a scientific partnership among the California Institute of Technology, the University of California and the National Aeronautics and Space Administration. The Observatory was made possible by the generous financial support of the W.M.

Keck Foundation. The authors wish to recognize and acknowledge the very significant cultural role and reverence that the summit of Mauna Kea has always had within the indigenous Hawaiian community. We are most fortunate to have the opportunity to conduct observations from this mountain.

[NASA Spacegrant tag-line] [Any others?]

REFERENCES

- Baptista, R. et al. 1998, MNRAS, 300, 233
- Beuermann, K. & Reinsch, K 2008, A&A, 480, 199
- Cushing W. D. et al. 2005, ApJ, 623, 1115
- Dhillon, V.S., & Marsh, T.R. 1995, MNRAS, 275, 89
- Dhillon, V.S., Littlefair, S.P., Howell, S.B., Ciardi, D.R., Harrop-Allin, M.K., & Marsh, T.R. 2000, MNRAS, 314, 826
- Harrison, T. E. et al. 2005, ApJ, 632, 123
- Harrison, T.E., Osborne, H.L. & Howell, S.B. 2004, AJ, 127, 3493
- Harrison, T.E., Osborne, H.L. & Howell, S.B. 2005, AJ, 129, 2400
- Harrison, T.E., Bornak, J., Howell, S.B., Mason, E., Szkody, P., & McGurk, R. 2009, AJ, 137, 4061
- Howell, S. B., Szkody, P. & Cannizzo, J. K. 1995, ApJ, 439, 337
- Howell, S.B., Nelson, L.A. & Rappaport, S. 2001, ApJ, 550, 897
- Howell, S.B., Harrison, T.E., & Szkody, P. 2004, ApJ, 602, L49
- Howell, S. B. 2005, The Astrophysics of Cataclysmic Variables and Related Objects , 330, 67
- Howell, S.B., Harrison, T.E., Szkody, P. 2010, AJ in press, astro-ph 1002.3428
- Ishioka, R., Sekiguchi, K., & Maehara, H. 2007, PASJ, 59, 929
- Knigge, C. 2006, MNRAS, 373, 484

- Mason, E., Skidmore, W., Howell, S. B., & Mennickent, R. E. 2001, *ApJ*, 563, 351
- Mauche, C. W. et al. 2009, *IBVS*, 5876, 1
- McLean, I. S. et al. 1998, *Proc. SPIE*, 3354, 566
- Mennickent, R. E., & Diaz, M. P. 2002, *MNRAS*, 336, 767
- Mennickent, R. E., Diaz, M. P. & Tappert, C. 2004, *MNRAS*, 347, 1180
- Moorwood, A. et al. 1998, *The Messenger*, 94, 7
- O’Donoghue, D., & Soltynski, M. G. 1992, *MNRAS*, 254, 9
- Patterson J. 1998, *PASP*, 110, 1132
- Patterson, J. 2001, *PASP*, 113, 736
- Patterson, J. et al. 2003, *PASP*, 115, 1308
- Ritter H. & Kolb U. 2003, *A&A*, 404, 301 (update RKcat7.12, 2009)
- Schoembs, R., & Vogt, N. 1981, *A&A*, 97, 185
- Sion, E.M., Cheng, F.-H., Huang, M., Hubeny, I., & Szkody, P. 1996, *ApJ*, 471, L41
- Smith, A. J., Haswell, C. A. & Hynes, R. I. 2006, *MNRAS*, 369, 1537
- Tappert, C., Gänsicke, B.T., Schmidtbreick, L., Mennickent, R.E., & Navarrete, F.P. 2007, *A&A*, 475, 575
- Thorstensen, J. R. 2003, *AJ*, 126, 3017
- Wade, R. A. & Horne, K. 1988, *ApJ*, 324, 411
- Warner, B., O’Donoghue, D., & Wargau, W. 1989, *MNRAS*, 238, 73

Wood, J. et al. 1986, MNRAS, 219, 629

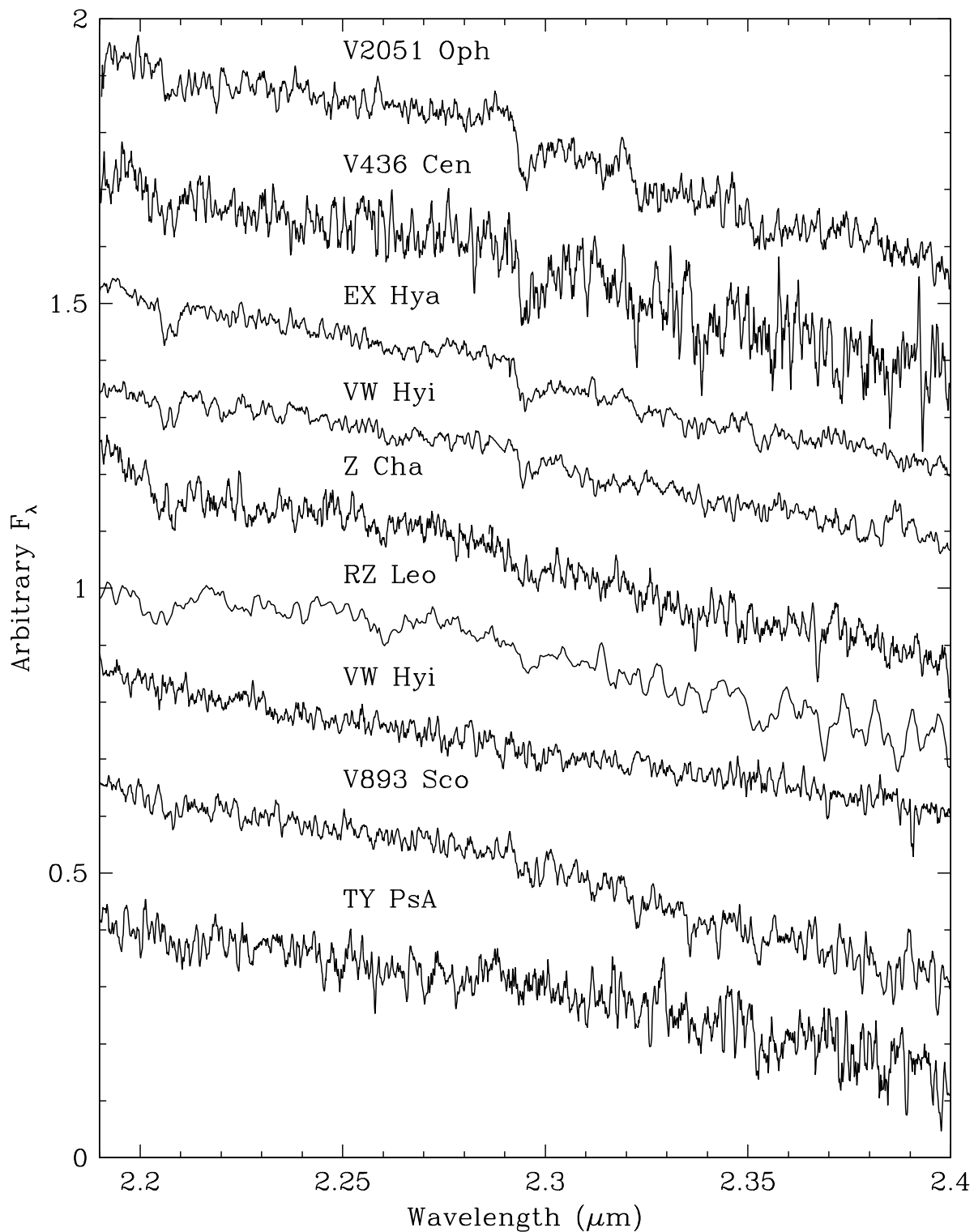


Fig. 1.— The VLT spectra of our program objects, except that for RZ Leo which was obtained using NIRSPEC on Keck II.

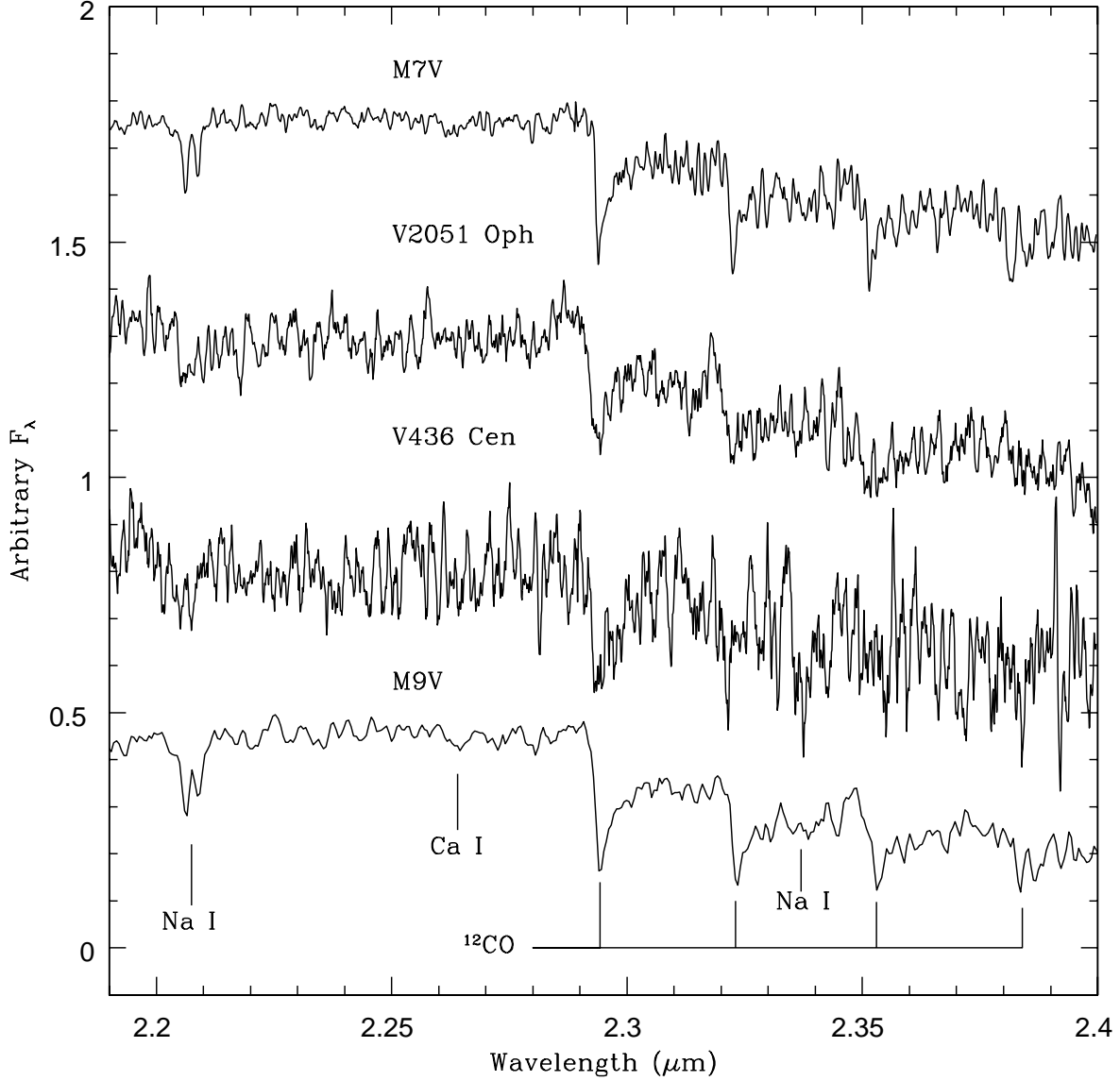


Fig. 2.— The spectra of V2051 Oph and V436 Cen compared to the spectra of two late-type templates an M7V (LHS 3003), and an M9V (LHS 2065, from the IRTF Spectral Library). The strongest absorption features, as used for spectral type determination, are indicated. The object spectra presented here have been vertically stretched for presentation purposes to more clearly demonstrate their similarity to the spectral type classification derived from the continuum subtracted data as described in the text. The lack of Ca I absorption, and the fact that the first overtone absorption of CO is stronger than the Na I doublet, indicate a very late spectral type. We estimate spectral types of M7 for V2051 and M8 for V436 Cen.

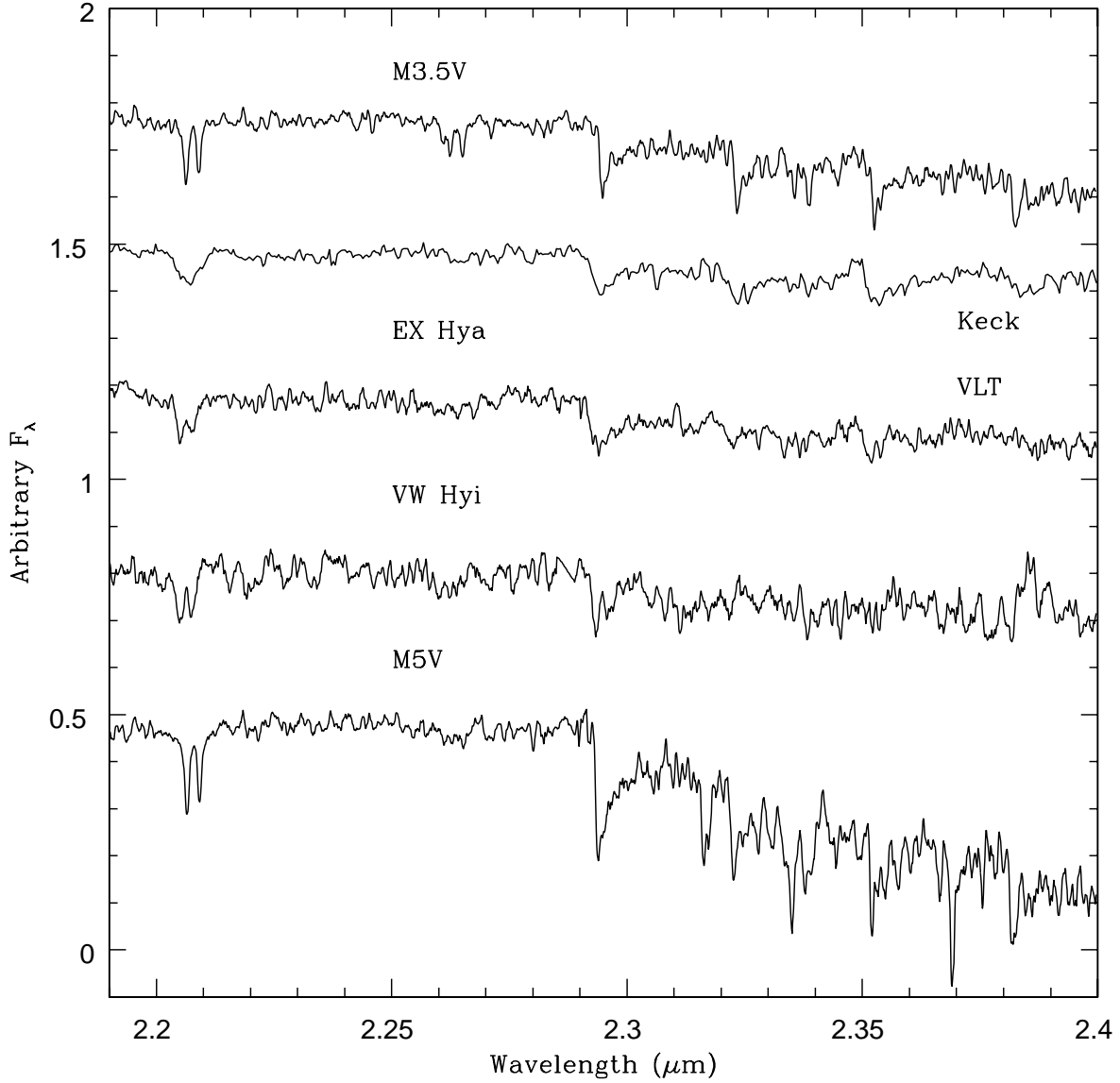


Fig. 3.— The spectra of the intermediate polar EX Hya, and the SU UMa system VW Hya, compared to the spectra of two mid-M dwarfs (the M3.5V is LHS 427, and the M5V template is LHS 2347). EX Hya was observed with both Keck (upper spectrum) and with the VLT (lower spectrum). As in Fig. 2, the object spectra have been stretched for presentation purposes. The relative strengths of Ca I triplets indicate spectral types near M5 for EX Hya, and M4 for VW Hya.

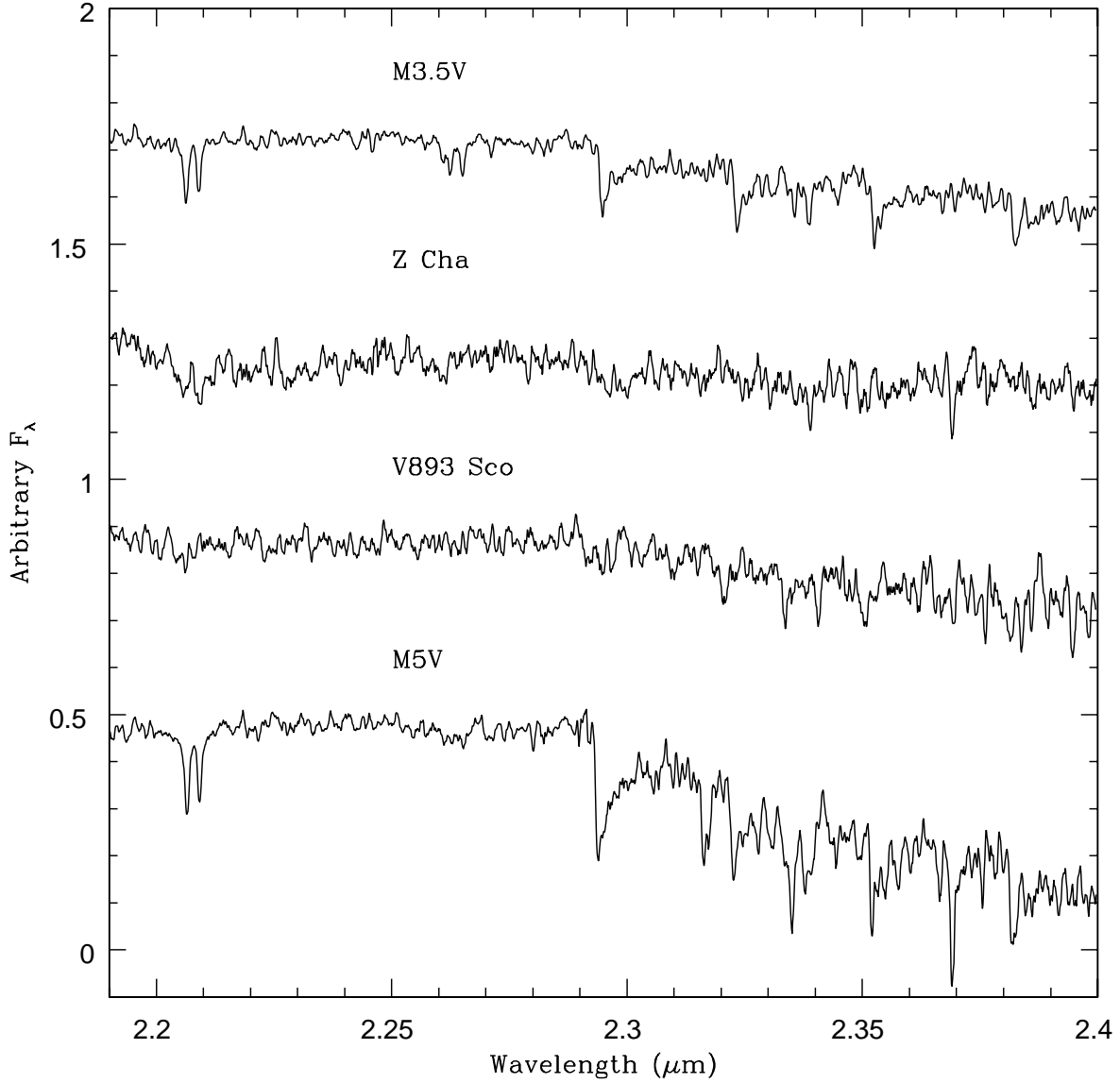


Fig. 4.— The stretched spectra of Z Cha and V893 Sco compared to two mid-M type templates. In Z Cha, the Na I doublet is clearly seen, as well as a hint of the Ca I triplet, suggesting a mid-M type secondary star. The CO features, however, are quite weak, suggesting a C deficit. The spectrum for V893 Sco is poorer, barely showing the Na I doublet, but it clearly has CO absorption, indicating that it has a slightly later spectral type than Z Cha. A later spectral type is also consistent with the obvious redward decline due to the presence of a water vapor absorption in V893 Sco.

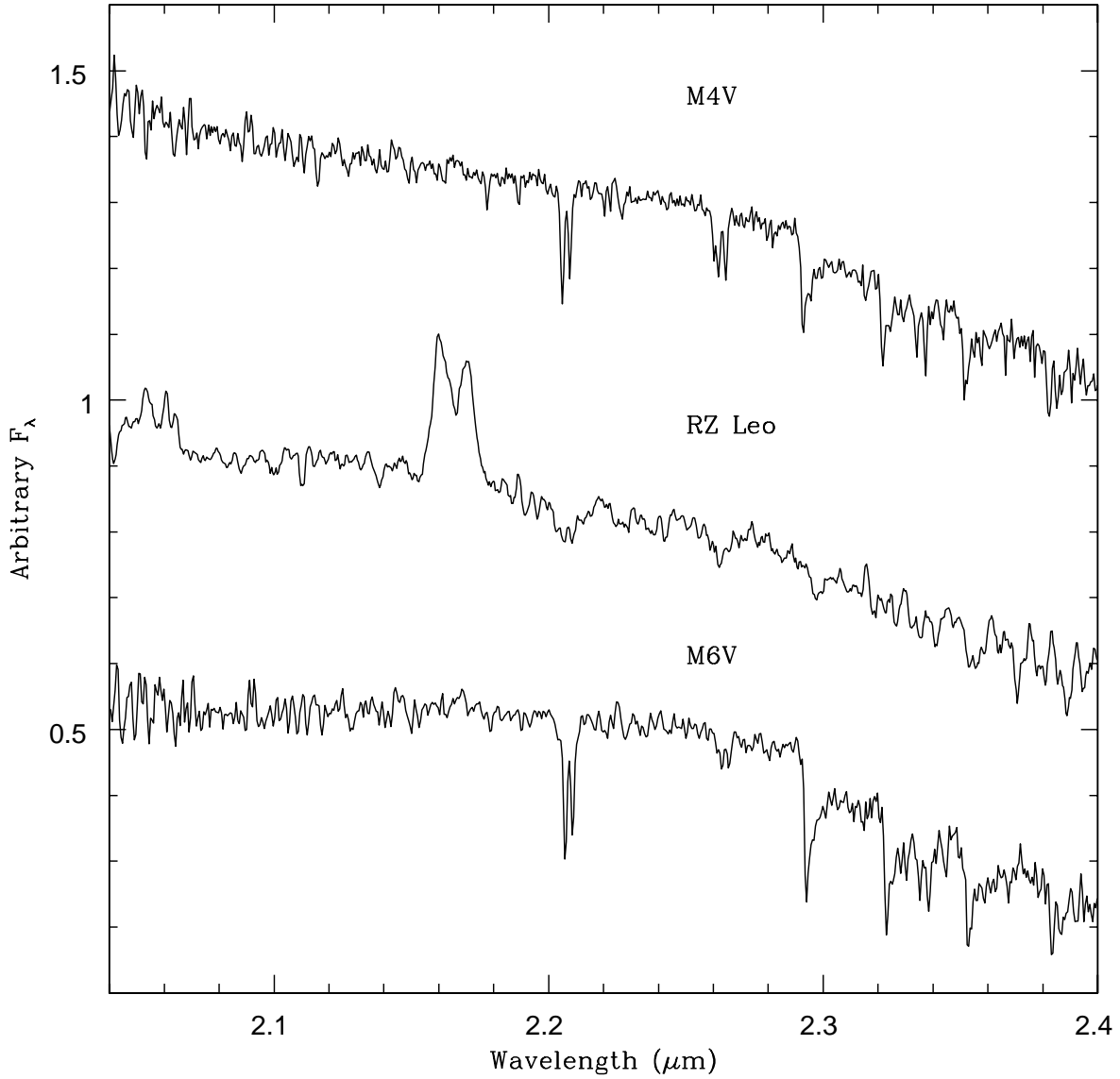


Fig. 5.— The NIRSPEC spectrum of RZ Leo compared to two mid-M type dwarfs (both from the IRTF Spectra library). The NIRSPEC data cover a larger range in wavelength (at lower spectral resolution) than the ISAAC spectra. The two strong emission lines are due to H I Br γ (at 2.16 μ m) and He I (at 2.06 μ m). The (unstretched) spectrum of RZ Leo clearly shows a strong decline due to water vapor. The strength of the first overtone of CO when compared to the depth of the sodium doublet, along with the strength of the Ca I triplet indicate a spectral type near M4.

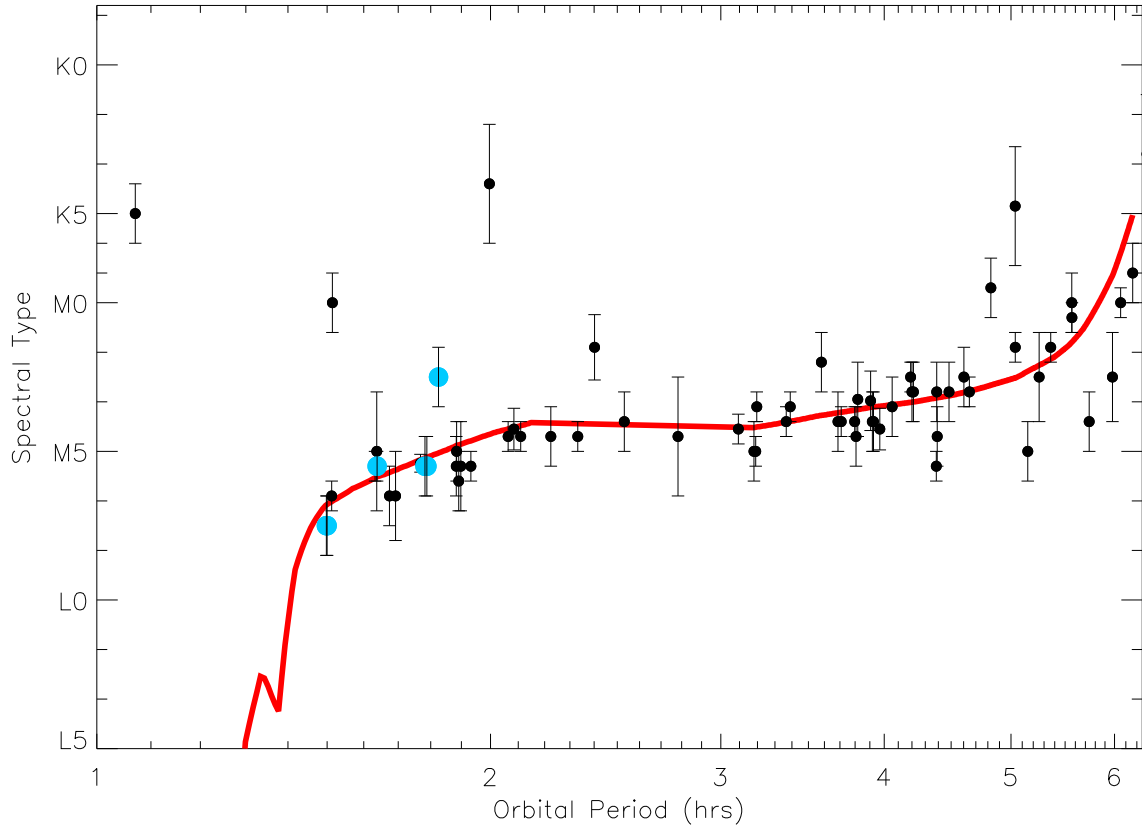


Fig. 6.— The Spectral type vs. P_{Orb} relationship from Knigge (2006) with the results from the analysis of the VLT ISAAC spectroscopy.

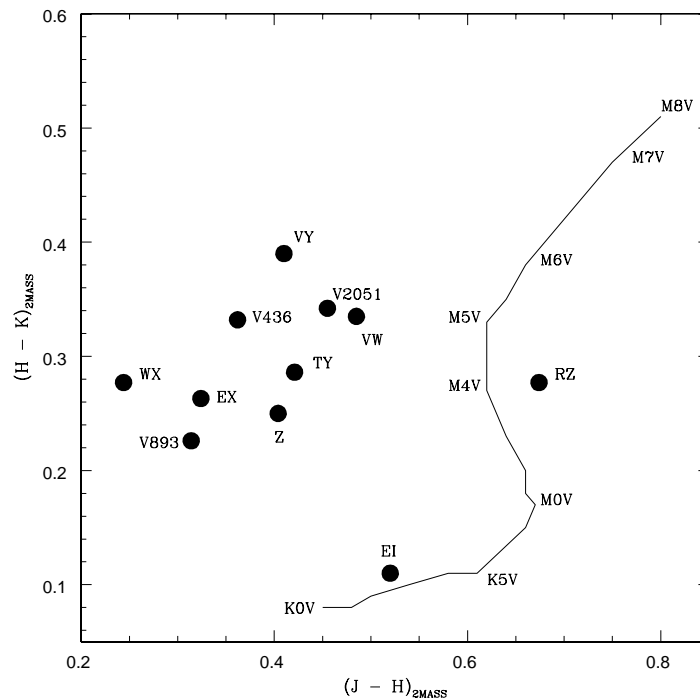


Fig. 7.— The infrared color-color plot for the program objects generated using the 2MASS data base. In addition, we have added two additional sub-gap CVs with detected secondaries, EI Psc and VY Aqr, using data from Harrison et al. (2009). Also shown is the main sequence color-color relationship (thin, label line) from K0V to M8V.

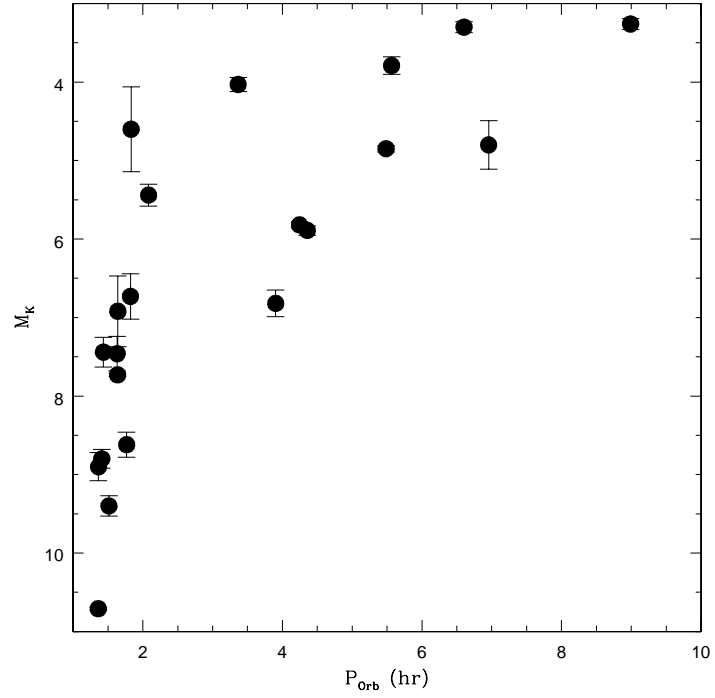


Fig. 8.— The M_K vs. P_{orb} relationship for cataclysmic variables with measured parallaxes (excluding “polars” and AM CVn systems).

Table 1. PROGRAM OBJECTS

System	Orbital Period (hrs)	Magnitude (m_k)	Primary Mass (M_\odot)	Secondary Mass (M_\odot)	Spectral Type	Inclination (degrees)
V2051 Oph	1.4982	13.530	0.78 ± 0.06	0.15 ± 0.03	...	83 ± 2
V436 Cen	1.5000	13.526	0.7 ± 0.1	0.17	...	65 ± 5
EX Hya	1.6376	11.69	0.790 ± 0.026	0.108 ± 0.008	M5-M6	77.8 ± 0.4
VW Hyi	1.7825	11.702	0.67 ± 0.22	0.11 ± 0.03	L0	...
Z Cha	1.7880	13.314	0.84 ± 0.09	0.125 ± 0.014	M5.5	81.1 ± 0.14
WX Hyi	1.7955	12.961	0.9 ± 0.3	0.16 ± 0.05	...	40 ± 10
V893 Sco	1.8231	12.68	0.89	0.17	...	72.5
RZ Leo	1.8249	15.387	M5	...
TY PsA	2.02	13.583
LHS 427	...	6.734	M3.5	...
LHS 2347	...	12.038	M5	...
LHS 3003	...	8.928	M7	...

Table 1. Program objects observed, listed in order of increasing orbital period.

Apparent magnitudes are K band as reported by 2MASS in the SIMBAD database. M star templates observed are listed as well. CV data were taken from Ritter & Kolb (2003, update 7.12).

Table 2. OBSERVATION LOG

System	Wavelength (μm)	Observation Date (UT)	Observation Time (Midpoint, UT)	Exp Time (s)	# Exp	Integration Time (s)	Phase Covered (%)
V2051 Oph	2.25	2008-05-12	07:51:30	70.0	30	2100	38.9
V2051 Oph	2.35	2008-05-12	08:54:18	70.0	30	2100	38.9
V436 Cen	2.25	2008-05-13	01:57:41	70.0	30	2100	38.9
V436 Cen	2.35	2008-05-13	00:54:22	70.0	30	2100	38.9
EX Hya (Keck)	2.21	2005-02-17	12:53:57	240.0	4	960	16.3
EX Hya	2.25	2008-06-21	02:00:42	25.0	36	900	15.3
EX Hya	2.35	2008-05-12	06:03:27	25.0	36	900	15.3
VW Hyi	2.25	2008-08-22	09:02:42	25.0	36	900	14.0
VW Hyi	2.35	2008-08-22	09:32:45	25.0	36	900	14.0
Z Cha	2.25	2008-09-17	09:12:36	50.0	36	1800	28.0
Z Cha	2.35	2008-05-10	23:31:41	50.0	36	1800	28.0
WX Hyi	2.25	2008-06-21	09:42:22	40.0	36	1440	22.3
WX Hyi	2.35	2008-06-21	08:47:54	40.0	36	1440	22.3
V893 Sco	2.25	2008-05-12	06:52:35	40.0	36	1440	21.9
V893 Sco	2.35	2008-05-10	06:39:43	40.0	36	1440	21.9
RZ Leo (Keck)	2.21	2007-03-05	12:21:43	240.0	12	2880	43.8
TY PsA	2.25	2008-06-20	08:04:50	70.0	30	2100	28.9
TY PsA	2.35	2008-06-20	06:59:29	70.0	30	2100	28.9
LHS 427	2.25	2008-07-18	02:55:00	8.0	64	512	...
LHS 427	2.35	2008-07-18	02:34:55	8.0	64	512	...
LHS 2347	2.25	2008-07-17	23:21:52	30.0	30	900	...
LHS 2347	2.35	2008-06-26	23:46:17	30.0	30	900	...
LHS 3003	2.25	2008-06-20	04:17:11	10.0	56	560	...
LHS 3003	2.35	2008-06-20	03:35:16	10.0	56	560	...

Table 2. All objects were observed at the VLT Antu telescope using ISAAC with the exception of RZ Leo & one observation of EX Hya as described in the text. The percent of phase covered does not include telescope overhead between exposures and therefore is a lower limit only.

Table 3. SPECTRAL TYPES AND INFRARED COLORS

System	Derived Spectral Type	Published Spectral Type	(J – H) _{2MASS}	(H – K) _{2MASS}	Reference
V2051 Oph	M7	...	0.46±0.05	0.34±0.06	...
V436 Cen	M8	...	0.36±0.04	0.33±0.05	...
EX Hya	M5	M5-M6	0.32±0.03	0.26±0.03	1
VW Hyi	M4	L0	0.49±0.03	0.34±0.03	2
Z Cha	M5	M5.5	0.40±0.05	0.25±0.05	3
RZ Leo	M4	M5	0.67±0.17	0.28±0.23	4
WX Hyi	0.24±0.03	0.28±0.04	...
V893 Sco	> M6	...	0.31±0.03	0.23±0.04	...
TY PsA	> M6	...	0.42±0.05	0.29±0.05	...

Table 3. Spectral types of program objects based on comparison to the IRTF spectral templates. References: (1) Beuermann & Reinsch (2008) (2) Mennickent et al. (2004) (3) Wade & Horne (1988) (4) Mennickent & Diaz (2002)